

PAPER • OPEN ACCESS

Rotationally inelastic processes of $C_2^-(^2\Sigma_g^+)$ colliding with He (1S) at low temperatures: *ab initio* interaction potential, state changing rates and kinetic modelling

To cite this article: B P Mant *et al* 2020 *J. Phys. B: At. Mol. Opt. Phys.* **53** 025201

View the [article online](#) for updates and enhancements.



IOP | ebooks™

Bringing together innovative digital publishing with leading authors from the global scientific community.

Start exploring the collection—download the first chapter of every title for free.

Rotationally inelastic processes of C_2^- ($^2\Sigma_g^+$) colliding with He (1S) at low temperatures: *ab initio* interaction potential, state changing rates and kinetic modelling

B P Mant¹ , F A Gianturco¹ , L González-Sánchez² , E Yurtsever³  and R Wester¹ 

¹Institut fuer Ionenphysik und Angewandte Physik, Universitaet Innsbruck, Technikerstr. 25, A-6020, Innsbruck, Austria

²Departamento de Química Física, University of Salamanca, Plaza de los Caídos sn, E-37008 Salamanca, Spain

³Department of Chemistry, Koç University, Rumelifeneriyolu, Sariyer, TR-34450, Istanbul, Turkey

E-mail: Francesco.Gianturco@uibk.ac.at

Received 27 June 2019, revised 18 October 2019

Accepted for publication 13 November 2019

Published 18 December 2019



CrossMark

Abstract

We discuss in detail the quantum rotationally inelastic dynamics of an important anion often discussed as a possible constituent of the interstellar medium (ISM) and in different environments of circumstellar envelopes: the C_2^- molecular ion. Its interaction forces with one of the most abundant atoms of the ISM, the neutral helium atom, are obtained for the first time using *ab initio* quantum chemistry methods. The overall angular anisotropy of the potential energy surface is analysed in order to link its features with the efficiency of transferring energy from the abundant He atoms to the internal rotational levels of this molecular anion. Calculations of the corresponding rotational state-to-state inelastic cross sections, for both excitation and de-excitation paths are obtained by using a multichannel quantum method. The corresponding inelastic rates at the temperatures of interest are determined and their role in distributing molecular states over the different populations of the rotational levels at the temperatures of that environment is discussed. These computed rates are also linked to the dynamical behaviour of the title molecule when confined in cold ion traps and made to interact with He as the common buffer gas, in preparation for state-selective photo-detachment experiments.

Supplementary material for this article is available [online](#)

Keywords: inelastic collisions, molecular anions, rate constants, buffer gas cooling


(Some figures may appear in colour only in the online journal)

1. Introduction

The diatomic carbon anion C_2^- is one of the most widely studied molecular anions which are stable in the gas phase.

The high electron affinity (EA) of neutral C_2 of around 3.3 eV [1, 2] results in the anion having well bound electronically excited states, of which two have been observed ($A^2\Pi_u$ and $B^2\Sigma_u^+$) [3] and are close in energy to the ground $X^2\Sigma_g^+$ state.

The spectroscopic properties of C_2^- have been studied for a long time in order to provide detailed information on its possible subsequent sighting in different environments of the interstellar medium (ISM). Absorption spectra for the $B^2\Sigma_u^+ \rightarrow X^2\Sigma_g^+$ transition were first observed by Herzberg and

 Original content from this work may be used under the terms of the [Creative Commons Attribution 3.0 licence](#). Any further distribution of this work must maintain attribution to the author(s) and the title of the work, journal citation and DOI.

Lagerqvist [4] who suggested it was due to the anion of the neutral C_2 molecule. Subsequent work by other researchers confirmed this suggestion [5–7] and since then many other spectroscopic and photodetachment experiments have been performed on this molecule [1, 2, 8–12] with the expressed aim of providing supporting information on its possible existence in diffuse molecular clouds.

Many high level theoretical studies of the C_2^- anion have also been carried out. Examples include calculations of the spectroscopic constants [13–17], potential energy curves [3, 14, 15, 17, 18], transition probabilities [14, 17, 18] and radiative lifetimes [18]. Recently Shi *et al* obtained impressive agreement between theory and experiment for spectroscopic parameters of six electronic states of the molecule and spin-orbit coupling constants for the $A^2\Pi_u$ state [19].

The neutral molecule C_2 is abundant in interstellar space [20] and comet tails [21]. It is also a common component of carbon stars [22, 23]. Combining these confirmed features of the neutral species with the fact that C_2 has indeed a large and positive EA, and that the C_2^- anion has strong absorption bands [7] which could specifically identify it, led to the expectation that the anion would then be rather likely to be detected in space [24]. Unfortunately, as yet no conclusive evidence of its presence has been found however, despite searches in carbon rich stars [25, 26] and diffuse molecular clouds [27], with only upper limits given to justify the lack of observation.

The interaction, and possible reaction, of C_2^- with other molecules of astrophysical interest has also been investigated to include its possible presence within more extended molecular networks to model molecular clouds. Barckholtz, Snow and Bierbaum [28] found that C_2^- (and longer C_n^- chains) are unreactive with H_2 at room temperature, while it is however rather reactive with atomic hydrogen in the process: $C_2^- + H \rightarrow C_2H + e^-$. Experiments in our group by Endres *et al* [29] also found that C_2^- is essentially unreactive with H_2 at room temperature but at 12 K some reactivity is observed with the most abundant molecule of the ISM.

The C_2^- anion is also of interest for ion trap experiments where, due to the anion's low lying electronic states with favourable Franck-Condon factors, it has been proposed as a candidate for laser cooling [30–32]. The simulations of Comparat *et al* has shown that C_2^- , initially cooled to tens of kelvin (using for example helium as a buffer gas [30]) could then be laser cooled to temperatures of milikelvin in ion traps. Laser cooled C_2^- could then be used to cool other negatively charged species in the same ion trap such as other anions [31] or even antiprotons [32] via sympathetic cooling. Very recently, Kas *et al* carried out a theoretical investigation of collisions of C_2^- with Li and Rb atoms [33], the latter of which is used in hybrid-trap experiments. By considering the anionic and neutral potential energy surfaces (PES), Kas *et al* concluded that the associative electron detachment (AD) process is not important for the ground electronic states of the involved partners but should be important for their interactions within their excited states. The authors also calculated the cross sections and corresponding thermal rate constants for rotationally inelastic collisions of Li and Rb with C_2^- ,

covering a low-energy range for the cross sections and obtaining the related rates up to 100 K.

In this paper we report inelastic scattering calculations for collisions of C_2^- in its ground electronic state ($^2\Sigma_g^+$) with helium since the rotational state-changing collisional processes of the molecular anion might be likely to occur with the He atom as a partner, given the diffuse presence of the latter in many different ISM environments. In particular, in the circumstellar envelope (CSE) around carbon rich stars where C_2^- could possibly be detected, He is around one fifth as abundant as H_2 and so is an important species for collisions in such environments. The rotationally inelastic cross sections which we calculate are in turn used to obtain the relevant thermal rate constants for rotational excitation (increasing angular momentum quantum number j) and de-excitation (lowering j) processes expected to occur in the range of temperatures of the molecular clouds and CSE envelopes where other carbon-rich anions have also been observed.

The state-changing rates obtained here for the first time can in turn be included within different chemical networks and databases (for example within the Basecol ro-vibrational collisional excitation database [34]) to improve on the modelling of their possible contributions to the populations of rotationally excited states of this anion reached via collisions with He occurring in diffuse interstellar clouds. Furthermore, the rates can be used to model cooling of C_2^- in ion traps (where helium is often used as a buffer gas) and to model the rotational population dynamics during photodetachment experiments [35]. Both aspects of the above possible processes involving the title molecular anion will be discussed later in the present work.

The paper is organised as follows. In section 2 we give the spectroscopic parameters of the C_2^- anion obtained from the literature. In section 3 we then present in some detail our new *ab initio* calculations of the interaction of C_2^- with He and report the representation of the interaction through the expansion of the PES in analytical form using a multipolar description of the latter in Legendre polynomials. This allows us to assess the spatial features of its overall anisotropy, linking it to the expected behaviour of the quantum state-changing cross sections. In section 4 we discuss our present quantum scattering calculations for the system which we have carried out using a coupled-channel (CC) description of the inelastic dynamics. In section 5 we present our results giving inelastic cross sections and rates, with the C_2^- molecule treated both as a doublet and pseudo-singlet target, a simplified coupling scheme that we shall explain further. Section 6 presents dynamical calculations which model the relaxation of C_2^- in an ion trap with helium buffer gas cooling and give specific suggestions about the expected behaviour of the initial rotational population collisional relaxation of the molecular anion under well specified trap parameters. Such quantities are obviously also of interest for preparing experimental setups which can describe the subsequent photodetachment processes involving the same initial anion. However, we will discuss and analyse this aspect of the problem in a separate paper currently under preparation. Finally, we offer conclusions in section 7.

Table 1. Experimental spectroscopic constants for the C_2^- in its ground $^2\Sigma_g^+$ electronic state. These constants are: R_e equilibrium bond length, B_e rotational constant, α_e rotational-vibrational coupling constant, ω_e harmonic frequency and χ_e and γ_e anharmonicity constants.

	Mead <i>et al</i> [8]	Reh fuss <i>et al</i> [9]
R_e (Å)	1.2684	1.268 31(13)
B_e (cm^{-1})	1.746 49(16)	1.746 66(32)
α_e (cm^{-1})	0.016 557(76)	0.016 51(46)
ω_e (cm^{-1})	1781.202(20)	1781.189(18)
$\omega_e\chi_e$ (cm^{-1})	11.6716(48)	11.6717(48)
$\omega_e\gamma_e$ (cm^{-1})	0.009 98(28)	0.009 981 28

2. Spectroscopic properties of the C_2^- molecule

For the sake of completeness, we give in table 1 the experimental Dunham expansion spectroscopic constants of the C_2^- in its ground ($^2\Sigma_g^+$) electronic state. Values for excited electronic states are given by Mead *et al* [8] and Reh fuss *et al* [9].

It is worth noting that since C_2^- is a homonuclear diatomic molecule, it does not exhibit a pure ro-vibrational spectrum and thus infrared adsorption or emission cannot be used for its detection. As discussed in the Introduction, transitions to and from the well characterised relatively low lying excited electronic states could however allow for the direct detection of the anion in different ISM environments.

3. *Ab initio* calculation of the PES

The interaction energy between C_2^- ($^2\Sigma_g^+$) and He (1S) was calculated *ab initio* on a Jacobi grid with R (the distance from the centre of mass of C_2^- to the He location) ranging from 2.8 to 20 Å and θ (the angle between R and the C_2^- internuclear axis) from 0° to 90° in 5° intervals. The C_2^- anion bond length was frozen at its equilibrium value of 1.268 Å [19]. Energies were calculated using the CCSD(T) method [36, 37] applied to unrestricted Hartree–Fock wavefunctions. All *ab initio* calculations were carried out using the Gaussian09 programme suite [38]. Before selecting the basis set, it is customary to check the convergence of results. In order to show this convergence of CCSD(T) results for the C_2^- –He surface, we present an example in table 2 for the basis set superposition error (BSSE) corrected (using the counterpoise procedure [39]) and uncorrected potential energy values at $\theta = 90^\circ$ and $R = 4.2$ Å. Correcting the BSSE using the counterpoise procedure in CCSD(T) calculations with our final basis set (the last row in table 2) was not computationally prohibitive and we have used this basis to calculate the presently employed PES. BSSE corrections obviously tend to diminish as the basis sets are increased; however, it is still not negligible at the level used in our PES calculations. The aug-cc-pV5Z basis on helium was necessary to reduce the BSSE to an acceptable level. For small values of $R < 3$ Å where the potential is repulsive, some calculations did not converge.

Energies for these geometries were obtained by fitting a Morse type function to the energies for each angular cut and extrapolating to small R . In total a grid of 551 *ab initio* energies were calculated.

The PES was analytically represented by expanding it using a Legendre polynomial series as

$$V(r_{\text{eq}}|R, \theta) = \sum_{\lambda}^{\lambda_{\text{max}}} V_{\lambda}(r_{\text{eq}}|R)P_{\lambda}(\cos \theta), \quad (1)$$

where, because C_2^- is a homonuclear target and thus symmetric around $\theta = 90^\circ$, only even terms of the Legendre series are required with integer label λ . Using a nine term expansion, i.e. with $\lambda_{\text{max}} = 16$, gave a root mean square error (RMSE) to the *ab initio* data of 0.78 cm^{-1} . The expansion parameters $V_{\lambda}(r_{\text{eq}}|R)$ are provided in the supplementary information and are available online at stacks.iop.org/JPB/53/025201/mmedia. The convergence of this fit with respect to the *ab initio* grid was checked. Carrying out the fit using a smaller grid with 10° intervals resulted in a less than 1% change for the most important V_0 and V_1 terms and RMSE of 2 cm^{-1} , hence our *ab initio* grid is sufficiently dense for an accurate PES fit.

The radial coefficients for $\lambda = 0, 2, 4, 6$ are plotted in figure 1. The V_0 term has a minimum of around -25 cm^{-1} at 4.5 Å while the other coefficients are mostly repulsive: the interaction of the anion with a He atom is thus found to be chiefly repulsive with only a weak attractive region due to the interplay of dispersion and polarisation effects. It is interesting to compare the present findings with recent calculations involving the same molecular anion but interacting instead with open-shell, highly polarisable systems. For these systems, there is a far stronger interaction of the same C_2^- molecular partner with Li and Rb, with the V_0 terms having minima of around 12 000 (1.5 eV) and 8000 cm^{-1} (1.0 eV) respectively, as discussed in detail by [33]. It should be noted however, that the crucial feature of the present PES is the extent and strength of its spatial anisotropy around the anionic target. It will be shown below that rotational excitation/de-excitation collisional efficiency is mainly linked to the overall spatial torque applied to the rotating molecule by the incoming He partner during the quantum dynamics which samples that feature of the interaction.

An overview of the PES is given as a contour plot in figure 2. The PES is relatively isotropic but becomes repulsive at slightly further distances for linear geometries versus perpendicular. The attractive interaction is relatively weak with the minimum in energy of around -30 cm^{-1} (relative to zero at infinite separation) at about 4.5 Å. The PES presented here can also be compared to the C_2H^- ($^1\Sigma$)–He (1S) system which we have recently investigated [35]. They show, in fact, nearly the same well depth at around 4.5 Å, although the C_2H^- –He PES has its minimum occurring off the perpendicular (T-shaped) configuration, a feature due to the lower symmetry of the former anion compared with the present case.

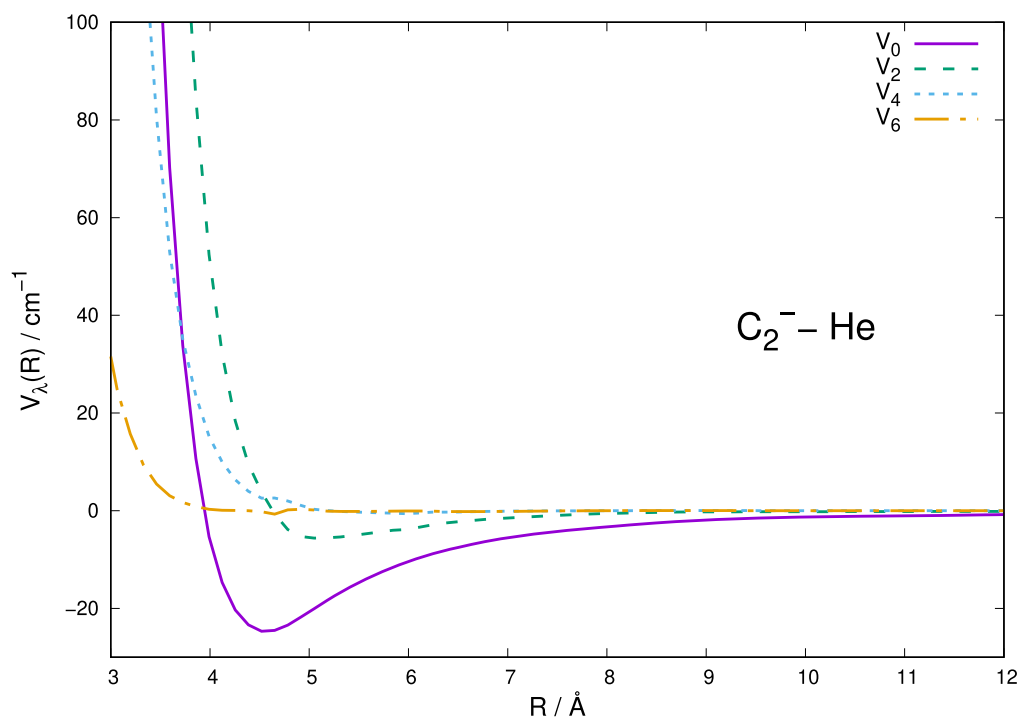


Figure 1. Computed radial coefficients of the expansion in equation (1) for $C_2^- (^2\Sigma_g^+)$ interacting with $He (^1S)$. Only the first four, most important radial functions are shown.

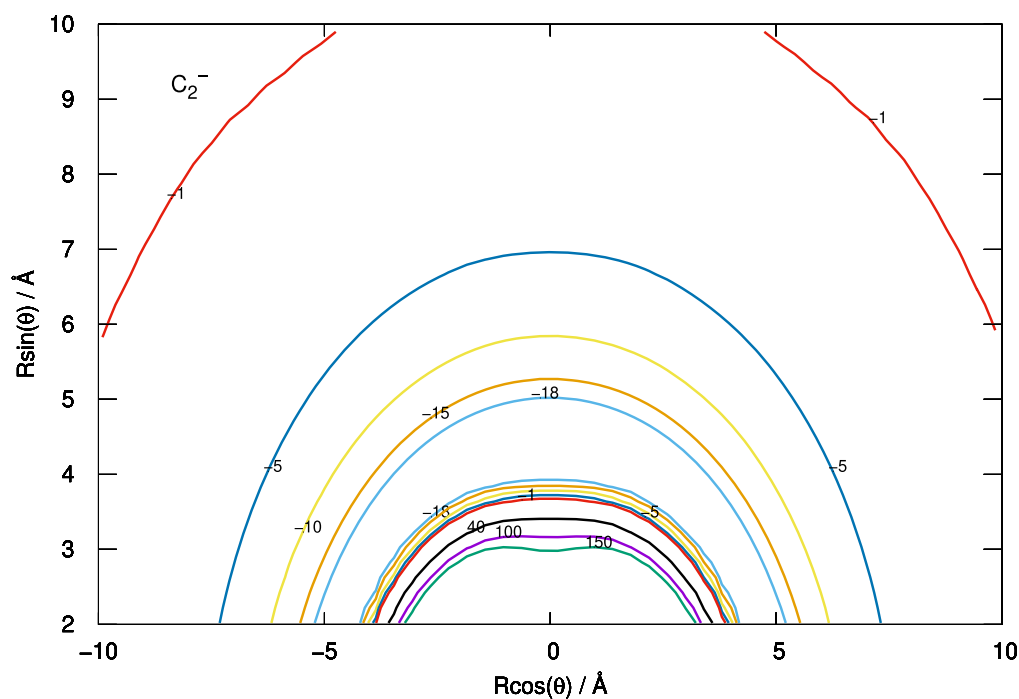


Figure 2. Contour plot of $C_2^- (^2\Sigma_g^+)$ - $He (^1S)$ PES projected onto Cartesian coordinates. Energies in cm^{-1} .

Table 2. Tests of basis sets [40] and BSSE corrections for C_2^- -He for geometry $\theta = 90^\circ$ and $R = 4.2 \text{ \AA}$.

Basis for C	Basis for He	V after BSSE correction (cm^{-1})	BSSE V(cm^{-1})
aug-cc-pVDZ	aug-cc-pVDZ	-19.24	14.30
aug-cc-pVTZ	aug-cc-pVTZ	-25.36	4.84
aug-cc-pVQZ	aug-cc-pVQZ	-26.90	4.31
aug-cc-pVQZ	aug-cc-pV5Z	-27.37	3.41

4. Scattering calculations at low temperatures

Quantum scattering calculations for the collision of C_2^- and He were carried out using our in-house quantum scattering computational code ASPIN [41]: in the present application the anion was treated as a rigid rotor (RR), since we are interested in the behaviour of rotational state-changing collisional processes. The validity of the RR approximation for the calculation of cross sections and rates of rotationally inelastic transitions for collisions energies of up to thousands of wavenumbers has been justified many times. The rotational-vibrational coupling has been shown to be small for H_2^+-He collisions [42] and essentially negligible for $SO + He$ [43] and $CS + He$ [44]. Lique even showed that including the reactive channels in $H + HCl$ collisions had very little effect on the rotationally inelastic cross sections [45].

The ground electronic state of C_2^- is $^2\Sigma_g^+$, a doublet state. The scattering of a structureless particle from a $^2\Sigma$ state target [46] is also implemented in our scattering code ASPIN. The presence of the electronic spin in a doublet state splits the usual nuclear rotational levels N of a rotating molecule into doublets so that each resultant rotational level j (other than $j = 0.5$) is split into two values with $j = N \pm 0.5$. The energy of the rotational levels are given as

$$\epsilon_{jN} = \begin{cases} BN(N+1) + \frac{1}{2}\gamma N & j = N + \frac{1}{2} \\ BN(N+1) - \frac{1}{2}\gamma(N+1) & j = N - \frac{1}{2} \end{cases}, \quad (2)$$

where B is the rotational constant taken as 1.74 cm^{-1} [19] and the spin-rotation constant, γ was taken from experiment with a value of $4.25 \times 10^{-3} \text{ cm}^{-1}$ [9].

ASPIN makes use of the CC method to solve the Schrödinger equation for scattering of an atom with a diatomic molecule. The method has been described in detail before [41, 47] and only a brief summary will be given here. For a given total angular momentum $\mathbf{J} = \mathbf{l} + \mathbf{j}$ the scattering wavefunction is expanded as

$$\Psi^{JM}(R, \Theta) = \frac{1}{R} \sum_{j,l} f_{jl}^J(R) \mathcal{Y}_{jl}^{JM}(\hat{\mathbf{R}}, \hat{\mathbf{r}}), \quad (3)$$

where l and j are the orbital and rotational angular momentum respectively, $\mathcal{Y}_{jl}^{JM}(\hat{\mathbf{R}}, \hat{\mathbf{r}})$ are coupled-spherical harmonics for l and j which are eigenfunctions of J . The values of l and j are constrained, via Clebsch–Gordan coefficients, such that their resultant summation is compatible with the total angular momentum J [41, 47]. $f_{jl}^J(R)$ are the radial expansion functions which need to be determined. Substituting the expansion into the Schrödinger equation with the Hamiltonian for atom-diatom scattering [41, 47] leads to the CC equations for each J

$$\left(\frac{d^2}{dR^2} + \mathbf{K}^2 - \mathbf{V} - \frac{\mathbf{I}^2}{R^2} \right) \mathbf{f}^J = 0. \quad (4)$$

Here each element of $\mathbf{K} = \delta_{ij} 2\mu(E - \epsilon_i)$ (where ϵ_i is the channel asymptotic energy), μ is the reduced mass of the system, $\mathbf{V} = 2\mu\mathbf{U}$ is the interaction potential matrix between channels and \mathbf{I}^2 is the matrix of orbital angular momentum.

The CC equations are propagated outwards from the classically forbidden region to a sufficient distance where the scattering matrix \mathbf{S} can be obtained. The rotational state-changing cross sections are obtained as

$$\sigma_{j \rightarrow j'} = \frac{\pi}{(2j+1)k_j^2} \times \sum_J (2J+1) \sum_{l,l'} |\delta_{jl,l'j'} - S_{jl,l'j'}^J|^2. \quad (5)$$

For doublet-state scattering, the above CC equations are modified by also coupling the projection of the spin angular momentum S with projection Σ on the internuclear axis [46]. The rotational basis functions in equation (3) are changed to explicitly include the spin term. The main result of this is to modify the analytical solutions of the potential matrix elements in equation (4) such that the Wigner 3- j symbols explicitly account for the electronic spin. The working equations for doublet-state scattering are given in the ASPIN publication [41] while a detailed derivation and discussion of the procedure implemented in ASPIN was given by Corey and McCourt [48]. The explicit treatment of collisions accounting for the doublet nature of the C_2^- molecule gives rise to spin-flip transitions in which the j quantum number changes but N stays the same.

To converge the CC equations, a rotational basis set was used which included up to $j = 20.5$ within the CC expansion. This choice provides 21 rotational functions in total which are directly included within the scattering wavefunction expansion. The CC equations were propagated between 1.7 and 90.0 Å in 2000 steps using the log-derivative propagator [49] up to 60 Å and the variable-phase method at larger distances [50] up to 90 Å. The convergence of the scattering calculations with respect to basis set, grid points, PES expansion, propagation distance and number of steps was checked. The cross sections are converged to at least a few percent or better which will have a negligible effect on calculated rates. The potential energy was interpolated between calculated $V_\lambda(r_{\text{eq}}|R)$ values using a cubic spline and extrapolated from the end of the *ab initio* grid at 20 Å as $V(R) = -\alpha_{\text{He}}/2R^4$ where $\alpha_{\text{He}} = 1.383 a_0^3$ [51] to account for the correct perturbative expansion of the long range interaction [52]. This part of the scattering propagation up to the asymptotic region was carefully checked because of its crucial importance when low temperature scattering processes are considered, as in the present study. It was found that the cross sections were essentially insensitive (again to a few percent or better) to the extrapolated form of the potential since the *ab initio* grid already went out to 20 Å where the interaction is of the order of -0.1 cm^{-1} , two orders of magnitude lower than the lowest scattering energy considered here.

Scattering calculations were carried out for collision energies between 1 and 1000 cm^{-1} using steps of 0.1 cm^{-1} for energies up to 100 cm^{-1} , 0.2 cm^{-1} for $100\text{--}200 \text{ cm}^{-1}$, 1.0 cm^{-1} for $200\text{--}500 \text{ cm}^{-1}$ and 2 cm^{-1} for $500\text{--}1000 \text{ cm}^{-1}$. This fine energy grid was used to ensure that important features such as resonances appearing in the cross sections were accurately accounted for and their contributions correctly included when

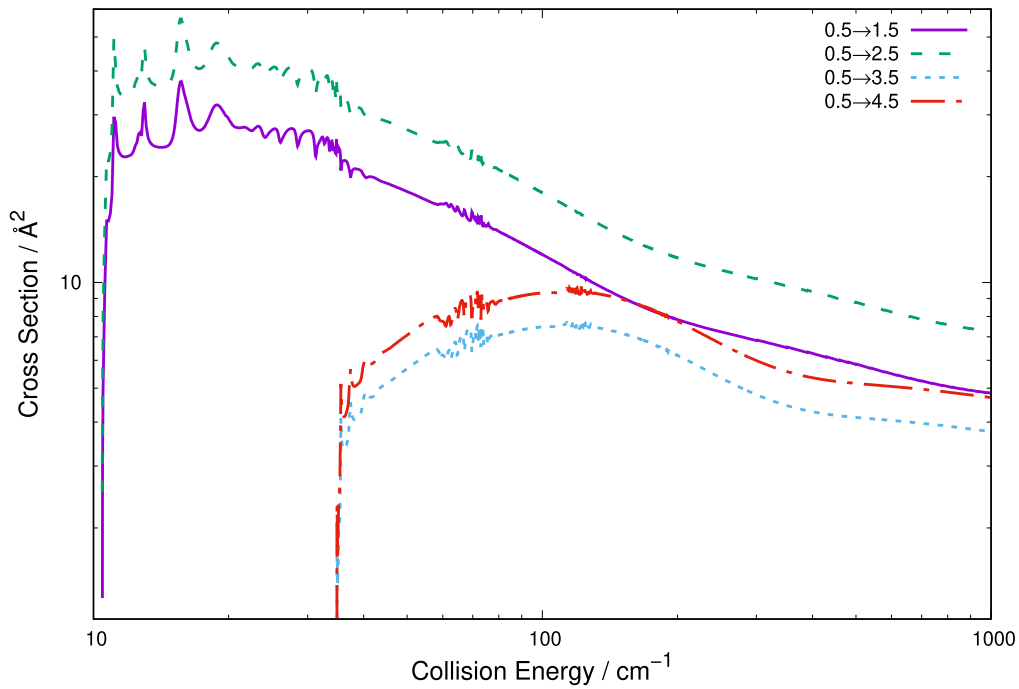


Figure 3. Examples of excitation cross sections for C_2^- -He scattering from ground $j = 0.5$ state.

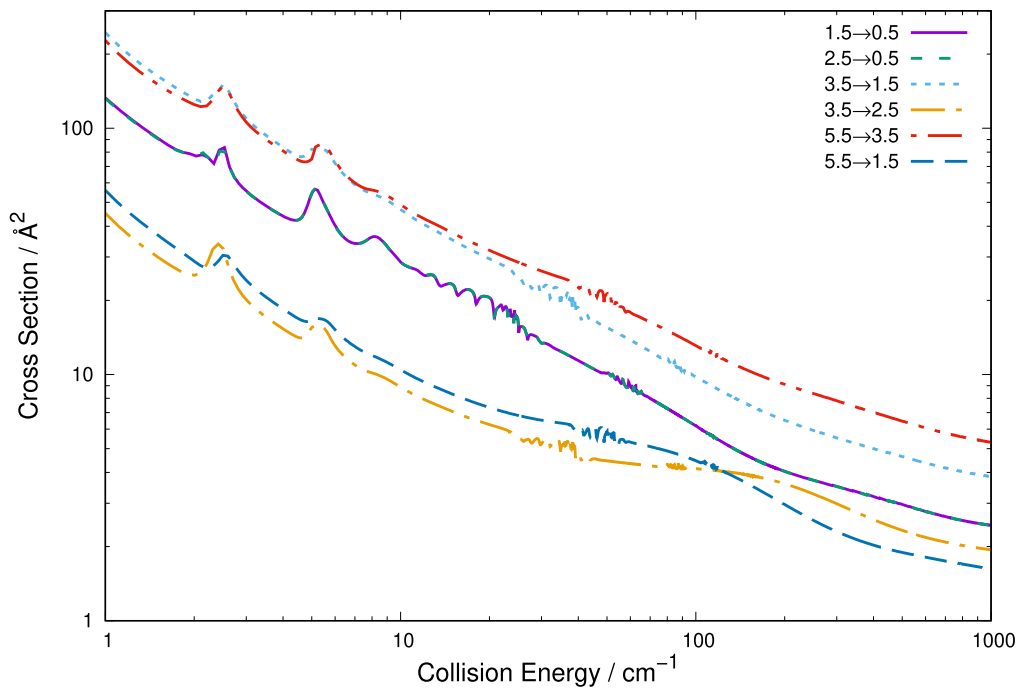


Figure 4. Examples of de-excitation cross sections for C_2^- -He scattering.

the corresponding rates were calculated. The number of partial waves was increased with increasing energy reaching $J = 89.5$ for the highest energies considered. Inelastic cross sections were computed for all transitions between $j = 0.5$ to $j = 8.5$ which should be sufficient to model buffer gas dynamics in a cold trap up to about 100 K, see below. The same levels are expected to be those most significantly populated during low-energy collisional exchanges with He atoms within ISM environments.

5. Results: features of cross sections and rates

Examples of the behaviour of the inelastic scattering cross sections are shown in figures 3–5 which illustrate various aspects of the system’s behaviour under energy-transfer scattering events. Figure 3 shows the inelastic scattering cross sections for rotational excitations from the ground $j = 0.5$ state to the $j = 2 \pm 0.5$ and $j = 4 \pm 0.5$ states. In both cases

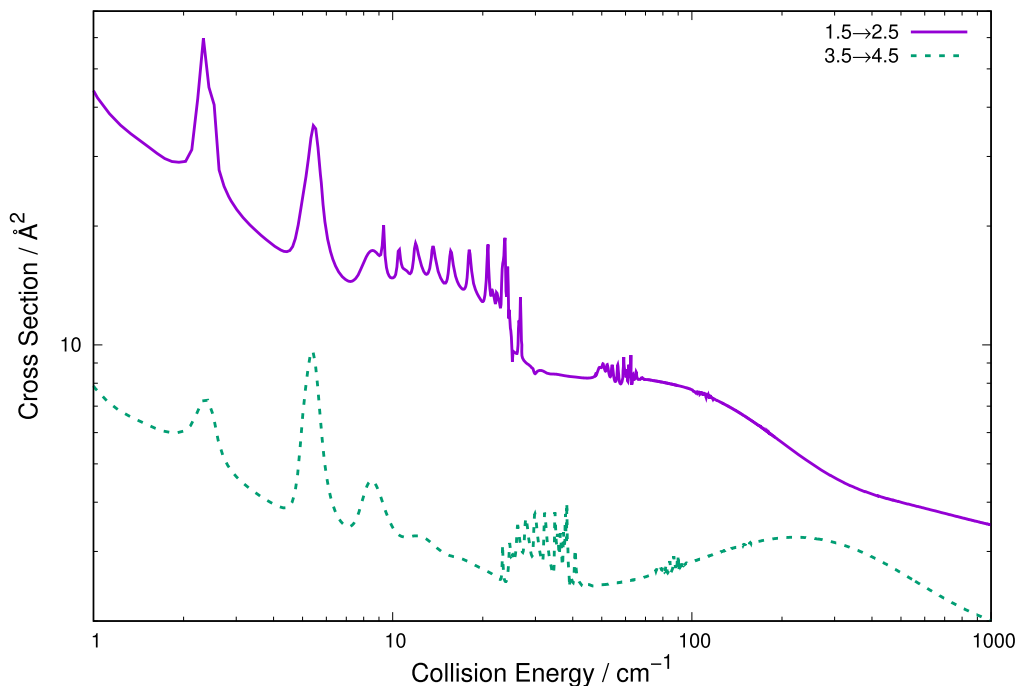


Figure 5. Examples of Spin-flip cross sections for $N = 2$ and $N = 4$ states.

the $N + 0.5$ states have larger cross sections. It can be seen that at lower collision energies the cross sections have a rich structure with many resonances. We observe, in fact, that between collision energies going from 10 up to around 40 cm^{-1} there are many resonant features in the cross sections, with further resonant structure appearing between 60 and 80 cm^{-1} . The most likely physical origins of such resonant features could be related either to dynamical trapping of the light He atom behind specific centrifugal barriers (broadly defined as ‘shape’ resonances) or to virtual excitation of the target molecule to low-lying rotational levels which become energetically closed at the collision energies in the asymptotic regions. These are usually classified as ‘virtual excitations’ or Feshbach resonances. In either case, we did not consider this as of interest in the present analysis, due to the current lack of experimental data on inelastic scattering processes, to further investigate the two types of resonances, while we have made sure that they all correctly contribute to the final size of the computed inelastic rates, especially in the threshold regions.

Figure 4 shows examples of de-excitation cross sections and illustrates a number of aspects of doublet-state scattering. The cross sections for $j = 2 \pm 0.5 \rightarrow j = 0.5$ are almost identical. This is expected since the interaction hamiltonian is spin-independent and both states end up in the same lower state, without any differences in the dynamical coupling acting during both types of collisions. This contrasts with the $j = 3.5 \rightarrow j = 2 \pm 0.5$ cross sections in figure 4 where it can be seen that the spin-conserving $j = 3.5 \rightarrow j = 1.5$ transition exhibits far higher cross sections than the corresponding spin-flip $j = 3.5 \rightarrow j = 2.5$ transitions. Also shown in the same figure are the $j = 5.5 \rightarrow j = 3.5$ and $j = 5.5 \rightarrow j = 1.5$ cross sections which follow the expected trend

of larger Δj transitions having smaller cross sections because of the increased energy gap involved in that inelastic process.

A final example for the C_2^- -He system is shown in figure 5 which shows two examples of cross sections for the spin-flip process within the same nuclear rotational level N . This process is either slightly endo or exoergic depending on the j state but can also be considered as an essentially elastic process for the purposes of buffer gas cooling.

In order to test the relative importance for the behaviour of the state-changing cross sections of treating the C_2^- molecule as a doublet system, scattering calculations were also carried out by treating the system instead as a pseudo-singlet ($^1\Sigma$). This constraint simplifies the dynamics as then only even j states are required in the calculations, due to the nuclear statistics of the $^{12}\text{C}_2^-$ molecule with zero spin nuclei. The scattering calculations discussed above were therefore repeated, this time treating the molecule as a singlet. The same basis set and energy grid were used and a similar increase of partial waves with energy was implemented in order to reach the same level of numerical convergence.

The excitation cross sections for the pseudo-singlet treatment of the C_2^- molecule are compared to those obtained by using the explicit doublet treatment and our present results are reported in figure 6. The relevant summed doublet cross sections are also shown for comparison. These are obtained by simply adding both cross sections for the same final N state but different j state, for example in figure 6 we show $\sigma_{0.5 \rightarrow 2.5} + \sigma_{0.5 \rightarrow 1.5}$ compared to $\sigma_{0 \rightarrow 2}$ for the singlet case. It can be seen that both calculations give very similar results, this being especially true at the higher energies we have considered. The similarity of the explicit $^2\Sigma$ treatment and pseudo- $^1\Sigma$ was also found in our previous work involving a much more strongly interacting system, where we analysed

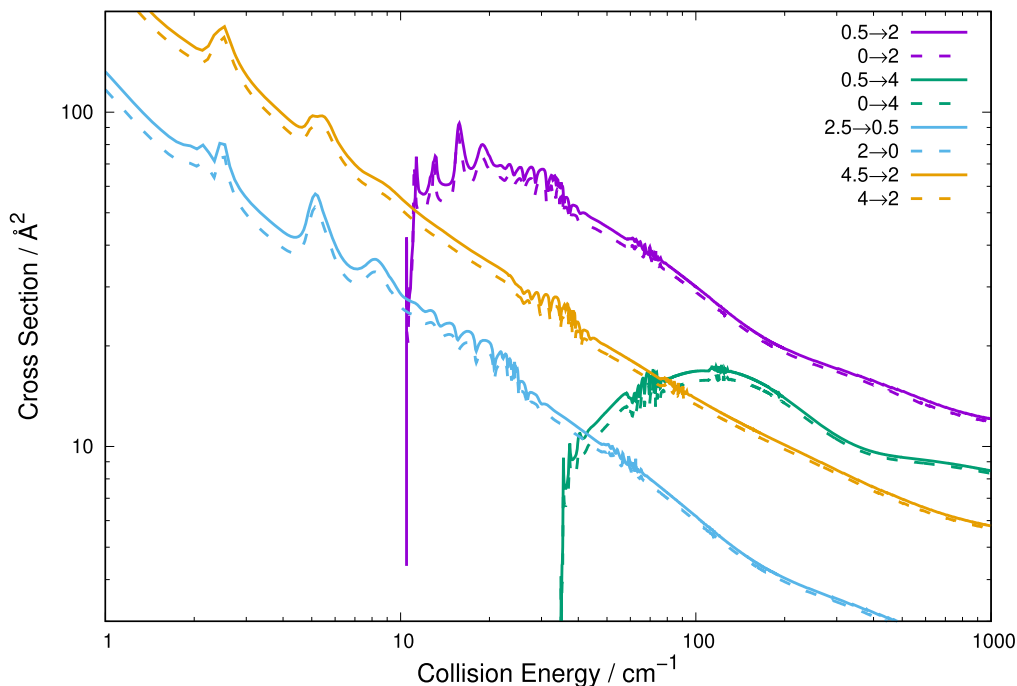


Figure 6. Comparison of excitation and quenching cross sections for pseudo-singlet treatment (dashed lines) versus explicit doublet (solid lines). For the doublet cross sections, the relevant cross sections were summed, see main text for details.

Table 3. Comparison of cross sections for summed doublet and pseudo-singlet treatment for the $0 \rightarrow 2$ transition. Cross sections in \AA^2 .

Energy (cm^{-1})	Summed doublet $\sigma_{0.5 \rightarrow 2}$	Pseudo-singlet $\sigma_{0 \rightarrow 2}$	Percentage difference
10.5	27.1	22.1	22%
30.0	67.4	62.5	8%
50.0	45.4	42.8	6%
100.0	30.0	29.0	3%
500.0	14.6	14.2	3%
1000.0	12.1	11.9	2%

the inelastic scattering of the H_2^+-He system with regards to the same state-changing rotationally inelastic collisions [53]. Such results indicate that, when analysing the quantum dynamics of rotationally inelastic collisions, such processes are essentially driven by the spatial anisotropic features of the scattering potential while the effects of spin-rotation coupling terms only cause rather minor changes on the efficiency of the considered transitions.

To compare the results between the singlet and doublet treatment more quantitatively, table 3 shows the numerical values and percentage difference for the $j = 0/0.5 \rightarrow j = 2$ transition cross sections at various energies. As the collision energy increases the difference between explicit doublet and pseudo-singlet treatment decreases. This occurs because as the scattering energy is increased, the differences between the pseudo-singlet and doublet terms in the \mathbf{V} matrix become negligible with respect to the \mathbf{K} matrix elements in the CC equations (equation (4)) which drive the magnitudes of the inelastic cross sections. The doublet terms are then essentially

given as a ratio of the pseudo-singlet values, scaled by the relevant Wigner $3-j$ symbols.

Even at the lowest energies considered where there is considerable resonance structure in the cross sections, the difference is still only around 20%. Such findings bear well for the use of the present decoupling scheme whereby the doublet electronic state of the target molecule can realistically be treated as if it were simply another case of a closed-shell, singlet electronic state of the anion, when one wishes to produce extensive information on the size and energy-dependence of rotationally inelastic, state-changing cross sections with a considerable reduction of computational complexity.

From the computed inelastic cross sections which we have discussed above, we can progress to the rotationally inelastic rate constants $k_{j \rightarrow j'}(T)$, which can be evaluated as the convolution of the computed inelastic cross sections over a Boltzmann distribution of the relative collision energies of the interacting partners as

$$k_{j \rightarrow j'}(T) = \left(\frac{8}{\pi \mu k_B^3 T^3} \right)^{1/2} \times \int_0^\infty E \sigma_{j \rightarrow j'}(E) e^{-E/k_B T} dE, \quad (6)$$

where all quantities are given in atomic units. The rate constants for all transitions considered in the previous discussion were therefore computed between 5 and 100 K, a range of temperatures for which we found the corresponding range of collision energies between 0 and 1000 cm^{-1} was numerically sufficient to converge the final rate values. In the supporting information we give the rates for all transitions between $j = 0.5$ to $j = 8.5$ and $j = 0$ and $j = 8$ for explicit doublet

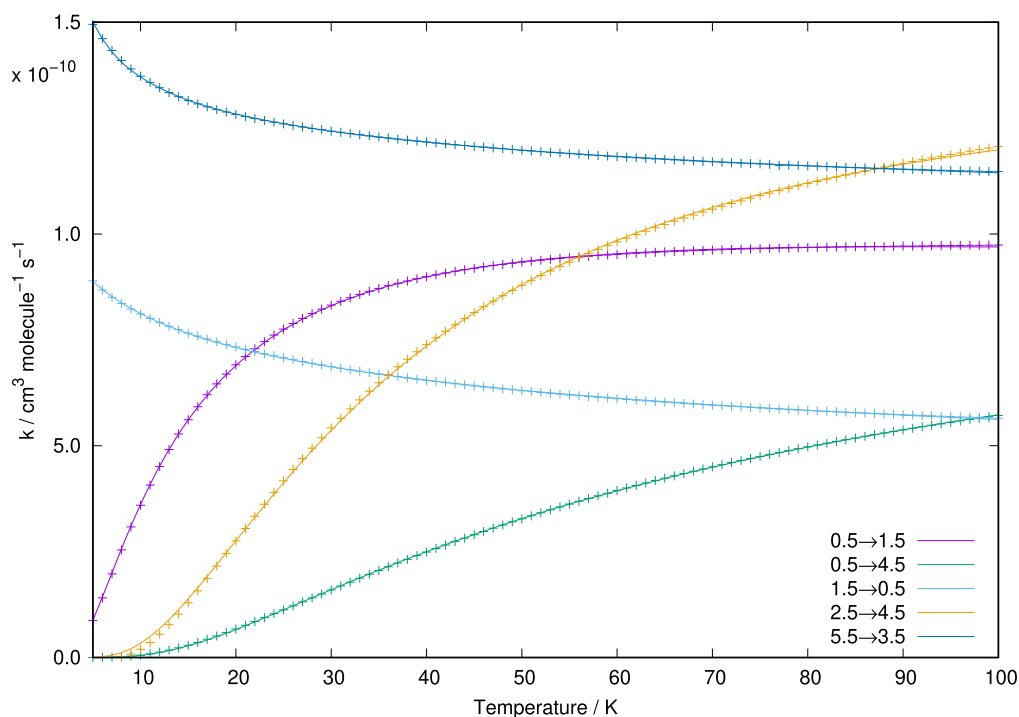


Figure 7. Rate constants $k_{j \rightarrow j'}(T)$ for various transitions of C_2^- colliding with He. Crosses are calculated rates, lines are least squares fit of equation (7) to rates. See main text for details.

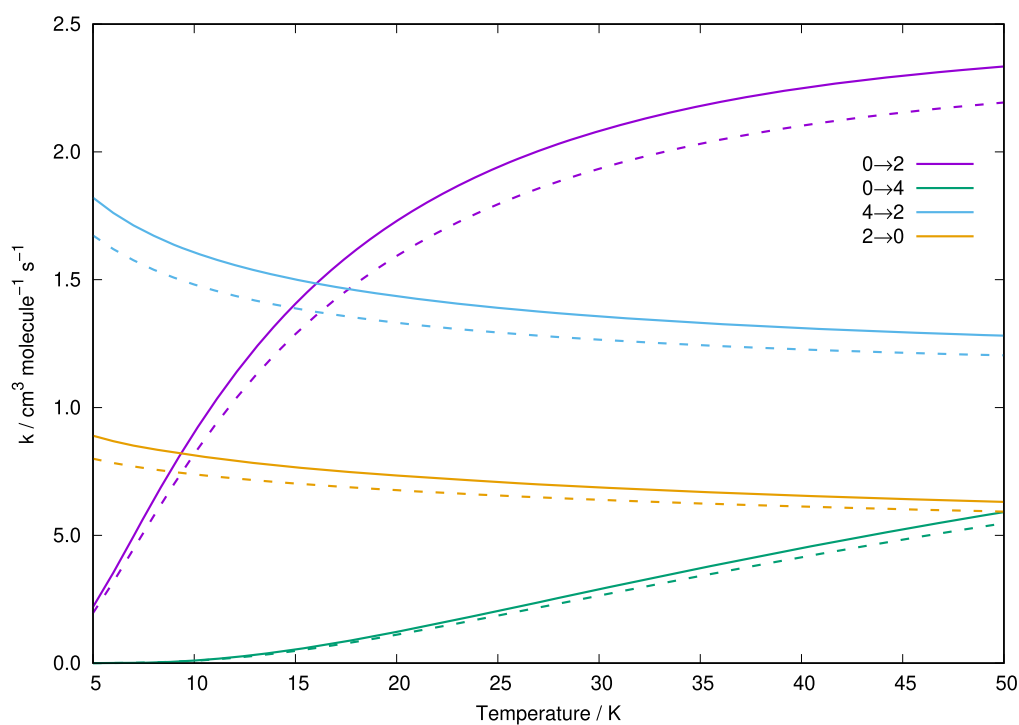


Figure 8. Rate constants $k_{j \rightarrow j'}(T)$ for various transitions involving C_2^- colliding with He, comparing results from the pseudo-singlet approximation (dotted lines) with those obtained from the summed components obtained for the doublet rates (solid lines). N labelling is used.

and pseudo-singlet treatment of the C_2^- anion respectively in 1 K intervals.

Examples of rate constants for both excitation (increasing j) and quenching (decreasing j) state-changing processes are shown in figure 7. As expected, at low temperatures the

corresponding quenching rates are larger than the excitation rates while, as the temperature increases, both types of rates become comparable in size.

To further compare the pseudo-singlet and explicit doublet treatment of C_2^- -He collisions, figure 8 compares the

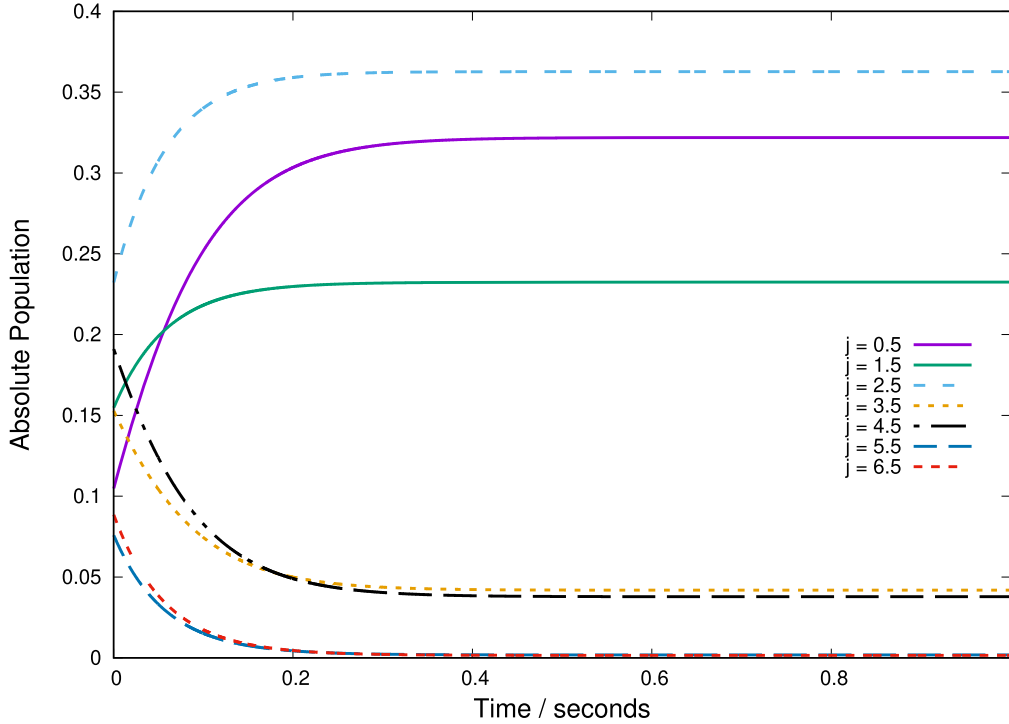


Figure 9. Thermalisation of $C_2^- (^2\Sigma^-)$ rotational state in collisions with He buffer gas at 15 K and density $\eta_{\text{He}} = 10^{11} \text{ cm}^{-3}$.

rate constants for each approach. Rates for the doublet treatment were added in the same manner described above. Both approaches give very similar rate constants, only differing by less than 10%.

It is interesting to note, as a comparison with earlier calculations involving the same molecular anion, that the rates and cross sections for collisional excitation and quenching of C_2^- by He atoms are found to be around one order of magnitude smaller than those obtained earlier for collisions of the same molecular anion with Rb and Li atoms, both being open-shell, strongly polarisable atomic partners [33]. The results reported in that work behave as expected since the C_2^- -He interaction is much weaker in strength and less orientation-dependent in terms of the size of its multipolar expansion coefficients.

The rates for both the explicit doublet and pseudo-singlet treatment were least squares fit to a three parameter function of form [54, 55]

$$k_{j \rightarrow j'} = \alpha(T/300)^\beta \exp(-\gamma/T) \quad (7)$$

which gives a good analytical representation of the rate constants. The lines in figure 7 connecting the calculated rates are an example of this function. In the supporting information we give values of the three fitting parameters as well as rms error for all of the rates considered in this work for pseudo-singlet and explicit doublet treatment of the C_2^- anion respectively. This analytical form gives the rates with minimal data and can be used, with caution, to extrapolate rates to higher temperatures than explicitly calculated here. This parametric representation is therefore chiefly provided for the use and inclusion of the presently calculated rotational

state-changing rates within larger ISM chemical networks containing a broad range of chemical processes (e.g. the KIDA database [55]).

6. Relaxation dynamics in cold ion traps

The rates discussed in the previous section can also be used to analyse the population dynamics of C_2^- during He collisions. This study therefore allows for the modelling of the possible operating conditions of cold ion traps where buffer gas cooling is carried out using helium, a buffer atom which has been successfully used in many experiments to obtain specific rotational state distributions for the trapped ions [56]. The master equations one needs to solve are given by

$$\frac{dn_i(t)}{dt} = \sum_{j \neq i} n_j(t) C_{ji}(T) - n_i(t) \sum_{i \neq j} P_{ij}(T). \quad (8)$$

They are solved by using the collisional thermal rates obtained from the quantum dynamics of the previous sections at a specific given temperature and selected He density [53]. The $P_{ij}(T)$ are the rates for the destruction of the population of level i , while its formation rates are given by the $C_{ji}(T)$ coefficients. The coefficients are given as a function of the inelastic rate coefficients and the He density:

$$P_{ij}(T) = \eta_{\text{He}} k_{i \rightarrow j}(T), \quad (9)$$

$$C_{ji}(T) = \eta_{\text{He}} k_{j \rightarrow i}(T). \quad (10)$$

As a test of a few specific conditions in the present analysis, the initial population of the molecular anion was taken to be the Boltzmann value at 50 K with a helium gas density in the cold trap of $\eta_{\text{He}} = 10^{11} \text{ cm}^{-3}$, a typical value used in experiments within our group [35]. For the chosen buffer gas temperature of 15 K, only the $j = 0.5, 2.5$ and 1.5 states are significantly populated. Figure 9 shows the relaxation of the rotational states of C_2^- ($^2\Sigma$) over the examined time interval. The molecules reach their thermalised Boltzmann distributions well before one second at this selected value for this helium gas density. The behaviour is similar to that which we have already found for the case of another molecular anion, C_2H^- undergoing collisional thermalisation with He. That process turned out to occur on a similar timescale [35], as it is to be expected from the similarities in the PES anisotropic features and coupling strength. In a recent publication [35] we have also shown that the switching on of a laser causes photo-detachment of the anion's excess electron from specific rotational states by controlling the corresponding laser wavelength and therefore selecting different rotational states of the anion in the trap. These features of the photo-detachment process for the C_2^- anion will be discussed in relation to experiments in preparation in our laboratory, in a separate, future publication.

7. Conclusions

We have calculated the interaction potential of C_2^- with He by employing accurate *ab initio* methods and further used that interaction energy surface to construct an analytical representation of the latter. Using this formulation of the PES we have carried out CC quantum scattering calculations to describe the collision of C_2^- with He at energies of $0\text{--}1000 \text{ cm}^{-1}$, treating the diatomic as a rigid-rotor and therefore focussing on state-changing inelastic processes involving solely the rotational states of the target anion. When carrying out the quantum calculations we considered the C_2^- either in its explicit doublet electronic ground state ($X^2\Sigma^+$) or, in a simpler formulation, as a pseudo-singlet ($^1\Sigma$) state. Both treatments were found to give similar inelastic cross sections indicating that the simpler pseudo-singlet treatment is sufficient to realistically model rotationally inelastic collisions, thereby excluding fine-structure transitions when obtaining the final cross sections and importantly, also the corresponding inelastic rates at low temperatures.

Using the computed cross sections we thus obtained the relevant thermal rate constants for rotational excitation and quenching processes at temperatures between 0 and 100 K and fit a three parameter functional form to the rates. As an example of the use of the rate constants, we modelled the buffer gas cooling of C_2^- at 15 K with typical buffer gas density for the He partner. The relaxation time required to reach thermal equilibrium was found to be similar to what we had already estimated for another molecular anion with the same buffer gas atom: the C_2H^- -He system [35]. The rotational state changing rates computed here will be used to model cooling times in an ion trap and population dynamics

when a laser is used for photodetachment, in a similar manner to what we have described in detail for similar systems in a recent publication [35]. Such photodetachment experiments on C_2^- will soon be carried out in our group.

The rates we have obtained here can also be directly used to model the efficiency of exciting this molecular anion when interacting with He atoms and also its collisional quenching which would be in competition with its possible radiative emission from the collisionally excited rotational levels. The entire range of the computed rates has been fitted to a parametric representation and the parameters have been reported in two tables of the present work. Thus, making use of this easier representation of our computed rates could therefore allow their employment within more extended chemical networks where one also needs to model the efficiency of the inelastic collisions between C_2^- and the abundant helium atoms present in ISM environments such as diffuse interstellar clouds where carbon-rich molecular anions are usually observed [57].

Acknowledgments

All the numerical data pertaining to our parametric fitting of the computed PES and to the actual values of the computed cross sections are available on request from the authors. We further acknowledge the financial support of the Austrian FWF agency through research grant n. P29558-N36. One of us (LS-G) further thanks MINECO (Spain) for grants CTQ2015-65033-P and PGC2018-09644-B-100.

ORCID iDs

B P Mant  <https://orcid.org/0000-0002-3116-5364>
F A Gianturco  <https://orcid.org/0000-0003-3962-530X>
L González-Sánchez  <https://orcid.org/0000-0002-7800-5739>
E Yurtsever  <https://orcid.org/0000-0001-9245-9596>
R Wester  <https://orcid.org/0000-0001-7935-6066>

References

- [1] Jones P L, Mead R D, Kohler B E, Rosner S D and Lineberger W C 1980 *J. Chem. Phys.* **73** 4419
- [2] Ervin K M and Lineberger W C 1991 *J. Phys. Chem.* **95** 1167
- [3] Nichols J A and Simons J 1987 *J. Chem. Phys.* **86** 6972
- [4] Herzberg G and Lagerqvist A 1968 *Can. J. Phys.* **46** 2363
- [5] Milligan E D and Jacox M E 1969 *J. Chem. Phys.* **51** 1952
- [6] Frosch R P 1971 *J. Chem. Phys.* **54** 2660
- [7] Lineberger W C and Patterson T A 1972 *Chem. Phys. Lett.* **13** 40
- [8] Mead R D, Hefter U, Schulz P A and Lineberger W C 1985 *J. Chem. Phys.* **82** 1723
- [9] Rehfuss B D, Liu D J, Dinelli B M, Jagod M F, Ho W C, Crofton M W and Oka T 1988 *J. Chem. Phys.* **89** 129
- [10] Royen P and Zackrisson M 1992 *J. Mol. Spectrosc.* **155** 427
- [11] Bragg A E, Wester R, Davis A V, Kammrath A and Neumark D M 2003 *Chem. Phys. Lett.* **376** 767

- [12] Nakajima M 2017 *J. Mol. Spectrosc.* **331** 106
- [13] Barsuhn J 1974 *J. Phys. B: At. Mol. Phys.* **7** 155
- [14] Zeitz M, Peyerimhoff S D and Buenker R J 1979 *Chem. Phys. Lett.* **64** 243
- [15] Dupuis M and Liu B 1980 *J. Chem. Phys.* **73** 337
- [16] Watts J D and Bertlett R J 1992 *J. Chem. Phys.* **96** 6073
- [17] Šedivcová T and Špirko V 2006 *Mol. Phys.* **104** 1999
- [18] Rosmus P and Werner H J 1984 *J. Chem. Phys.* **80** 5085
- [19] Shi W, Li C, Meng H, Wei J, Deng L and Yang C 2016 *Comput. Theor. Chem.* **1079** 57
- [20] Lambert D L, Sheffer Y and Federman S R 1995 *Astrophys. J.* **438** 740
- [21] Lambert D L, Sheffer Y, Danks A C, Arpigny C and Magain P 1990 *Astrophys. J.* **353** 640
- [22] Souza S P and Lutz B L 1977 *Astrophys. J.* **216** L49
- [23] Lambert D L, Gustafsson B, Eriksson K and Hinkle K H 1986 *Astrophys. J. Suppl. Ser.* **62** 373
- [24] Vardya M S and Krishna Swamy K S 1980 *Chem. Phys. Lett.* **73** 616
- [25] Fay T and Johnson H R 1972 *PASP* **84** 284
- [26] Wallerstein G 1982 *Astron. Astrophys.* **105** 219
- [27] Civiš S, Hosaki Y, Kagi E, Izumiura H, Yanagisawa K, Šedivcová T and Kawaguchi K 2005 *Publ. Astron. Soc. Japan* **57** 605
- [28] Barckholtz C, Snow T P and Bierbaum V M 2001 *Astrophys. J.* **547** L171
- [29] Endres E S, Lakhmanskaya O, Hauser D, Huber S E, Best T, Kumar S S, Probst M and Wester R 2014 *J. Phys. Chem. A* **118** 6705
- [30] Yzombard P, Hamamda M, Gerber S, Doser M and Comparat D 2015 *Phys. Rev. Lett.* **114** 213001
- [31] Fesel J, Gerber S, Doser M and Comparat D 2017 *Phys. Rev. A* **96** 031401(R)
- [32] Gerber S, Fesel J, Doser M and Comparat D 2018 *New J. Phys.* **20** 023024
- [33] Kas M, Loreau J, Liévin J and Vaeck N 2019 *Phys. Rev. A* **99** 042702
- [34] Dubernet M L *et al* 2013 *Astron. Astrophys.* **553** A50
- [35] Gianturco F A, González-Sánchez L, Mant B P and Wester R 2019 *J. Chem. Phys.* **151** 144304
- [36] Purvis G D III and Bartlett R J 1982 *J. Chem. Phys.* **76** 1910
- [37] Pople J A, Head-Gordon M and Raghavachari K 1987 *J. Chem. Phys.* **87** 5968
- [38] Frisch M J *et al* 2009 Gaussian 09 Revision E.01 (Wallingford, CT: Gaussian Inc.)
- [39] Boys S F and Bernardi F 1970 *Mol. Phys.* **19** 553
- [40] Kendall R A, Dunning T H Jr and Harrison R J 1992 *J. Chem. Phys.* **96** 6796
- [41] López-Duráñ D, Bodo E and Gianturco F A 2008 *Comput. Phys. Commun.* **179** 821
- [42] Iskandarov I, Gianturco F A, Vera M H, Wester R, da Silva H Jr and Dulieu O 2017 *Eur. Phys. J. D* **71** 141–53
- [43] Lique F, Spielfiedel A, Dhont G and Feautrier N 2006 *Astron. Astrophys.* **458** 331
- [44] Lique F and Spielfiedel A 2007 *Astron. Astrophys.* **462** 1179
- [45] Lique F 2015 *J. Chem. Phys.* **142** 241102
- [46] Alexander M H 1982 *J. Chem. Phys.* **76** 3637
- [47] Arthurs A M and Dalgarno A 1960 *Proc. R. Soc. A* **256** 540
- [48] Corey G C and McCourt F R 1983 *J. Phys. Chem.* **87** 2723
- [49] Manolopoulos D E 1986 *J. Chem. Phys.* **85** 6425
- [50] Martinazzo R, Bodo E and Gianturco F A 2003 *Comput. Phys. Commun.* **151** 187
- [51] Masil M and Strarace A F 2003 *Phys. Rev. A* **68** 012508
- [52] Stone A 2013 *The Theory of Intermolecular Forces* (Oxford: Oxford University Press)
- [53] Hernández Vera M, Gianturco F A, Wester R, da Silva H Jr, Dulieu O and Schiller S 2017 *J. Chem. Phys.* **146** 124310
- [54] Satta M, Gianturco F A, Carelli F and Wester R 2015 *Astrophys. J.* **799** 228
- [55] Wakelam V *et al* 2015 *ApJS* **217** 20
- [56] Hauser D, Lee S, Carelli F, Spieler S, Lakhmanskaya O, Endres E S, Kumar S S, Gianturco F A and Wester R 2015 *Nat. Phys.* **11** 467
- [57] Millar T J, Walsh C and Field T A 2017 *Chem. Rev.* **117** 1765–95